Nitration and Oxidation of a Hydrophobic Tyrosine Probe by Peroxynitrite in Membranes: Comparison with Nitration and Oxidation of Tyrosine by Peroxynitrite in Aqueous Solution†

Hao Zhang, Joy Joseph, Jimmy Feix, Neil Hogg, and B. Kalyanaraman*

Biophysics Research Institute and Free Radical Research Center, Medical College of Wisconsin, Milwaukee, Wisconsin 53226

Received December 29, 2000; Revised Manuscript Received March 21, 2001

ABSTRACT: It has been reported that peroxynitrite will initiate both oxidation and nitration of tyrosine, forming dityrosine and nitrotyrosine, respectively. We compared peroxynitrite-dependent oxidation and nitration of a hydrophobic tyrosine analogue in membranes and tyrosine in aqueous solution. Reactions were carried out in the presence of either bolus addition or slow infusion of peroxynitrite, and also using the simultaneous generation of superoxide and nitric oxide. Results indicate that the level of nitration of the hydrophobic tyrosyl probe located in a lipid bilayer was significantly greater than its level of oxidation to the corresponding dimer. During slow infusion of peroxynitrite, the level of nitration of the membrane-incorporated tyrosyl probe was greater than that of tyrosine in aqueous solution. Evidence for hydroxyl radical formation from decomposition of peroxynitrite in a dimethylformamide/water mixture was obtained by electron spin resonance spin trapping. Mechanisms for nitration of the tyrosyl probe in the membrane are discussed. We conclude that nitration but not oxidation of a tyrosyl probe by peroxynitrite is a predominant reaction in the membrane. Thus, the local environment of target tyrosine residues is an important factor governing its propensity to undergo nitration in the presence of peroxynitrite. This work provides a new perspective on selective nitration of membrane-incorporated tyrosine analogues.

Biological nitration is a rapidly growing area of research in oxidative pathology (for a review on this subject, see ref *1*). 3-Nitrotyrosine (NO_2Tyr)[1] has been proposed as a diagnostic marker product for peroxynitrite ($ONOO^-$/ONOOH), nitrogen dioxide radical ($NO_2^\bullet$), and related reactive nitrogen species (*2*−*5*). NO_2Tyr has been detected in tissues associated with various pathophysiological conditions (*6*−*10*). Recently, Pfeiffer et al. (*11*, *12*) reported that nitration of tyrosine was negligible when tyrosine was incubated in solution with low concentrations of authentic $ONOO^-$ or with nitric oxide ($^\bullet NO$) and superoxide ($O_2^{\bullet -}$) that were cogenerated. Under these conditions, however, the major reaction product was reported to be dityrosine (DiTyr) formed from oxidation of tyrosine (*12*). The investigators also reported that nitration of tyrosine could be detected only in the presence of high concentrations (2 μM/s) of $ONOO^-$ (*12*). On the basis of these results, the authors questioned the use of NO_2Tyr as an in vivo marker of $^\bullet NO/O_2^{\bullet -}$ toxicity. Furthermore, the authors implicated DiTyr as a major in vivo marker product of $ONOO^-$/ONOOH (*12*).

It is well-established that $ONOO^-$ and 3-morpholinosydnonimine HCl (SIN-1) both cause extensive nitration of protein tyrosyl residues as compared to free tyrosine (*13*, *14*). Nitration efficiency was reported to be controlled by many factors, including the location and the hydrophobicity and/or hydrophilicity of tyrosine residues in a protein (*1*). Previously, we reported that both SIN-1 and $ONOO^-$ cause preferential nitration of γ-tocopherol in membranes compared to tyrosine in aqueous solution (*15*). The hydrophobic interior of the membrane increased the nitrating efficiency of peroxynitrite. Consequently, in vitro studies using "free" tyrosine in aqueous solution do not totally mimic the in vivo peroxynitrite-dependent nitration conditions. Thus, the conclusion that tyrosine nitration is not a biologically relevant product of peroxynitrite is premature (*11*, *12*). Very little information about the reaction between tyrosine or tyrosine analogues and peroxynitrite in a hydrophobic environment exists. This will be biologically relevant as peroxynitrite freely crosses the membrane bilayer. However, in a biological setting, many protein tyrosyl residues exist in the hydrophobic regions of membrane proteins or in the interior of proteins.

In this study, we have examined the nitration and oxidation of a membrane-incorporated hydrophobic tyrosine probe and

† This work was supported by National Institutes of Health Grants RR01008 and HL63119.

* To whom correspondence should be addressed: Biophysics Research Institute, Medical College of Wisconsin, 8701 Watertown Plank Rd., Milwaukee, WI 53226. Telephone: (414) 456-4035. Fax: (414) 456-6512. E-mail: balarama@mcw.edu.

[1] Abbreviations: BOC, *tert*-butyl pyrocarbonate; BTBE, *N*-*t*-BOC tyrosine *tert*-butyl ester; DiBTBE, 3,3′-di *N*-*t*-BOC tyrosine *tert*-butyl ester; DiTyr, 3,3′-dityrosine; DLPC, 1,2-dilauroyl-*sn*-glycero-3-phosphatidylcholine; DMF, *N*,*N*-dimethylformamide; DMPO, 5,5-dimethyl-1-pyrroline *N*-oxide; DMSO, dimethyl sulfoxide; DBNBS, 3,5-dibromo-4-nitrosobenzenesulfonic acid; DTPA, diethylenetriaminepentaacetic acid; EMPO, 5-ethoxycarbonyl-5-methyl-pyrroline *N*-oxide; ESR, electron spin resonance; NO_2-BTBE, 3-nitro *N*-*t*-BOC L-tyrosine *tert*-butyl ester; NO_2Tyr, 3-nitrotyrosine; $NaHCO_3$, sodium bicarbonate; $ONOO^-$ and ONOOH, peroxynitrite; SD, standard deviation; SIN-1, 3-morpholinosydnonimine HCl; 5-PCSL, 1-palmitoyl-2-stearoyl(5-doxyl)-*sn*-glycero-3-phosphocholine; 12-PCSL, 1-palmitoyl-2-stearoyl-(12-doxyl)-*sn*-glycero-3-phosphocholine; 16-PCSL, 1-palmitoyl-2-stearoyl(16-doxyl)-*sn*-glycero-3-phosphocholine.

10.1021/bi002958c CCC: $20.00
Published on Web 05/31/2001

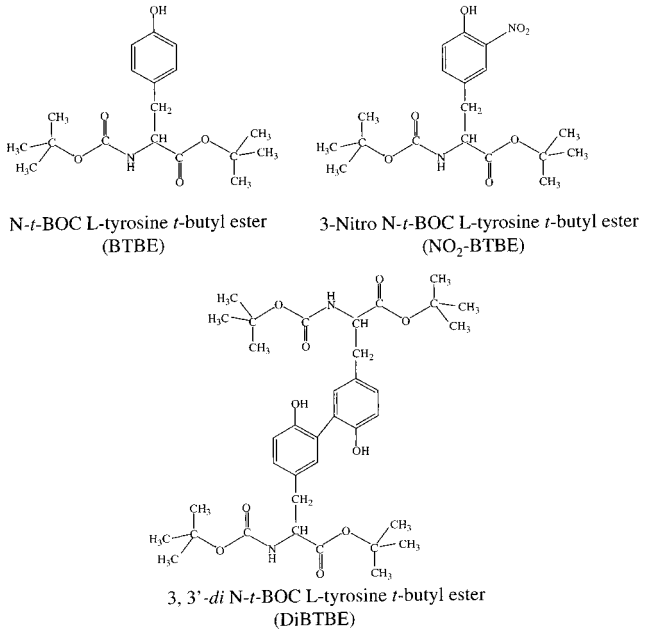

FIGURE 1: Structures of hydrophobic *N-t*-BOC L-tyrosine *tert*-butyl ester and its nitration and oxidation products.

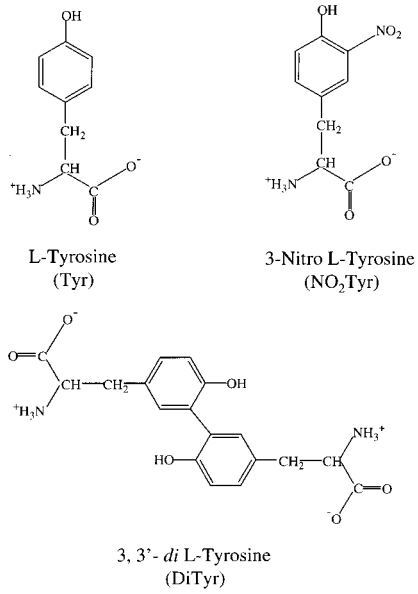

FIGURE 2: Structures of hydrophilic L-tyrosine and its nitration and oxidation products.

free tyrosine in aqueous solution. The rationale for this study is to investigate the effect of a hydrophobic environment on peroxynitrite-dependent nitration of tyrosine. We compared the peroxynitrite-dependent nitration and oxidation of L-tyrosine with that of *N-t*-BOC L-tyrosine *tert*-butyl ester (BTBE), a hydrophobic tyrosine analogue (Figures 1 and 2). Results indicate that at low concentrations, $ONOO^-$/ONOOH preferentially nitrated BTBE. In addition, nitration and oxidation of BTBE in the membrane was more efficient than nitration and oxidation of tyrosine in the aqueous solution. The results presented here indicate that nitration but not oxidation of tyrosyl residues is a major reaction pathway for peroxynitrite in membranes. Recent reports have shown that peroxynitrite is highly membrane permeable and reacts effectively with transmembrane targets (*16*−*18*). In line with these findings, we postulate a radical-mediated scheme for peroxynitrite-mediated oxidation and nitration of hydrophobic tyrosyl probes in the membrane (Scheme 1 in Discussion).

EXPERIMENTAL PROCEDURES

The following chemicals and enzymes were purchased from various sources as indicated: tyrosine, tyrosine methyl ester, tyrosine ethyl ester, hydrogen peroxide, sodium nitrite, sodium bicarbonate, and 3-nitrotyrosine (Sigma); tetranitromethane (Aldrich); tyrosine *tert*-butyl ester (Fluka); horseradish peroxidase (Boehringer Mannheim); SIN-1 (Cal-Biochem); and spin-labels (5-PCSL, 12-PCSL, and 16-PCSL) and 1,2-dilauroyl-*sn*-glycero-3-phosphatidycholine (DLPC) (Avanti Polar Lipids). DiTyr was prepared according to the published procedure (*19*). Peroxynitrite was synthesized according to the published procedure (*20*), and its concentration in 0.01 M NaOH was determined using the extinction coefficient ($\epsilon = 1670\ M^{-1}\ cm^{-1}$ at 302 nm). Both 5-ethoxycarbonyl-5-methylpyrroline *N*-oxide (EMPO) and 3,5-dibromo-4-nitrosobenzenesulfonic acid (DBNBS) were prepared according to the published procedures (*21*, *22*). All reagents were prepared in doubly distilled deionized water.

Syntheses of Compounds

N-t-BOC L-Tyrosine tert-Butyl Ester. L-Tyrosine *tert*-butyl ester (237 mg, 1 mmol) was dissolved in 10 mL of dioxane and kept cool in an ice bath. A solution of 106 mg of sodium carbonate was dissolved in 10 mL of water and the mixture added to the dioxane solution followed by the addition of a solution of 240 mg of *tert*-butyl pyrocarbonate in 5 mL of dioxane. The mixture was stirred in an ice bath for 1 h and acidified to pH 2−3 with hydrochloric acid. The mixture was then extracted with 3 × 20 mL of ethyl acetate, and the extract was treated with anhydrous Na_2SO_4 and evaporated to dryness. The resulting white solid was recrystallized from a 1:1 mixture of ethyl acetate and hexane (yield of 220 mg). The purity was ascertained by HPLC.

3-Nitro N-t-BOC L-Tyrosine tert-Butyl Ester (NO_2-BTBE). Tetranitromethane (60 mg) was mixed with 50 mg of BTBE in 4 mL of methanol. The reaction mixture was kept in the dark and stirred overnight at room temperature. The mixture was then mixed with 4 mL of phosphate buffer (0.1 M, pH 7.4) and extracted with 2 × 8 mL of chloroform. The chloroform layer was removed and dried under a stream of nitrogen gas. The crude product was redissolved in methanol and further purified in a C-18 preparative column (Beckman, 10 mm × 250 mm, 5 μm) using a methanol gradient, increasing the concentration from 70 to 78% over the course of 100 min. The retention times for BTBE and its nitro derivative (i.e., NO_2-BTBE) under these conditions were 35 and 56 min, respectively. Fractions containing NO_2-BTBE were pooled, extracted with chloroform, and dried under nitrogen gas. The purity of NO_2-BTBE was determined in a C-18 analytical HPLC column. Isocratic elution at 70% methanol for 30 min showed a single peak (11 min). No additional peak was detected upon elution with 100% methanol. The UV−vis spectral characteristics of the pure product were similar to those of NO_2Tyr. The UV−vis spectrum of NO_2-BTBE recorded in 70% methanol containing 15 mM phosphate (pH 3.0) exhibited an absorbance maximum at 354 nm. This absorbance maximum shifted to 424 nm (extinction coefficient = 4000 $M^{-1}\ cm^{-1}$) in 70% methanol containing 0.01 M NaOH.

3,3′-Di N-t-BOC L-Tyrosine tert-Butyl Ester (DiBTBE). BTBE (60 mg) was suspended in an 80 mL reaction solution containing 15% methanol and 50 mM acetate buffer (pH 4.7) and the mixture stirred for 30 min. Then 400 μL of hydrogen peroxide (30%) and 200 units of horseradish peroxidase were added to the BTBE solution, and the mixture was stirred at room temperature for 90 min. The reaction mixture was extracted twice with an equal volume of chloroform. The chloroform extracts were combined and dried under a stream of cold nitrogen gas. The dried extract was redissolved in methanol and separated in a C-18 preparative column (Beckman, 10 mm × 250 mm, 5 μm) pre-equilibrated with 77% methanol in 15 mM phosphate (pH 3.0) and eluted with a linear increase in methanol concentration from 77 to 80% over the course of 70 min. The retention times for BTBE and its dimer (i.e., DiBTBE) were 22 and 60 min, respectively. The fractions containing DiBTBE were pooled, extracted with chloroform, and dried with nitrogen gas. The purity of DiBTBE was verified using analytical HPLC.

Incorporation of BTBE into DLPC Liposomes

A methanolic solution of BTBE was added to DLPC dissolved in methanol. The mixture was then dried under a stream of nitrogen gas and kept in a vacuum desiccator overnight. Multilamellar liposomes were formed by thoroughly mixing the dried lipid in phosphate buffer (100 mM, pH 7.4) containing DTPA (100 μM). Unilamellar liposomes were prepared by five cycles of freezing and thawing using liquid nitrogen followed by five cycles of extrusion through a 0.2 μm polycarbonate filter (Nucleopore, Pleasanton, CA) in an extrusion apparatus (Lipex Biomembranes, Inc., Vancouver, BC). The efficiency of BTBE incorporation into DLPC liposomes was determined by measuring its amount in the supernatant of 30 mM DLPC liposomes containing 300 μM BTBE after centrifugation at 11 000 rpm for 30 min. Results showed that more than 98% of the BTBE was incorporated into the membrane.

HPLC Analysis of Tyrosyl Probes and Derivatives

A 200 μL reaction mixture containing liposomes was mixed with 200 μL of methanol and votexed for 1 min to dissolve the liposomes. The resulting solution was mixed with 400 μL of chloroform and 80 μL of NaCl (5 M), vortexed for an additional 2 min, and centrifuged at 5000 rpm for 10 min, and the top layer (aqueous phase) was removed. The chloroform layer was dried under a stream of nitrogen gas. The extract was redissolved in a 200 μL solution containing 70% methanol and 15 mM phosphate buffer (pH 3.0) for HPLC analysis. Extraction of authentic compounds BTBE (300 μM), NO_2-BTBE (50 μM), and DiBTBE (20 μM) in liposomes (30 mM DLPC) gave the following extraction efficiencies: 95.3 ± 1.4, 99.4 ± 0.7, and 101 ± 1.2% ($n = 3$).

The extract in 70% methanol and 15 mM phosphate buffer (pH 3.0) was injected into the HPLC system with a C-18 reverse-phase column (Partisil ODS-3, 250 mm × 4.6 mm, Alltech), eluted with a linear methanol increase (from 70 to 75%) in 15 mM phosphate (pH 3.0) for 30 min. UV detection at 280 nm was used to monitor the levels of BTBE and NO_2-BTBE. Detection limits of these compounds were 200 and 20 pmol, respectively. Fluorescence detection at 294 nm (excitation) and 401 nm (emission) was used to monitor the level of DiBTBE. The detection limit was 5 pmol. BTBE, its corresponding nitro derivative, and the dimer product were eluted at 8.3, 11, and 23 min, respectively. Repeat injections of authentic compounds showed no noticeable loss of these compounds under injection conditions over the course of 40 h at room temperature.

Similarly, tyrosine, NO_2Tyr, and DiTyr were separated on an HPLC system equipped with fluorescence and UV detectors (*23*) using a mobile phase of methanol and phosphate buffer (50 mM, pH 3.0) (4:96) for 30 min and a C-18 reverse-phase column (Partisil ODS-3, 250 mm × 4.6 mm, Alltech). UV detection at 280 nm was used to monitor the levels of tyrosine and NO_2Tyr, and fluorescence detection at 284 nm (excitation) and 410 nm (emission) was used to monitor the levels of DiTyr and higher oxidation products of tyrosine. The authentic standards (tyrosine, DiTyr, and NO_2Tyr) were eluted at 7.5, 9.5, and 17.5 min, respectively.

Peroxynitrite Infusion

The slow infusion of peroxynitrite was performed using an infusion/withdraw pump from Harvard Apparatus (model 966) under constant stirring of liposomes or aqueous solution containing tyrosine probes. Peroxynitrite (6.25 mM diluted in 0.25 M NaOH) was infused at a constant rate (8.0 ± 0.1 μL per 10 min) into 0.5, 0.75, 1, 2, and 4 mL of liposomes (30 mM DLPC containing 300 μM BTBE) until the final concentration of peroxynitrite was measured to be 50 μM. The infusion rates for peroxynitrite were 10, 6.7, 5.0, 2.5, and 1.3 μM/min, respectively. Measurement of pH levels of the reaction mixtures after infusion showed that the maximum pH shift was less than 0.1 unit. Peroxynitrite decomposition under these conditions was evaluated by following the absorption change at 302 nm and its nitration efficiency before and after infusion. After 45 min, the changes in optical absorption and nitration efficiency after infusion were less than 5% of the starting peroxynitrite stock solution.

Mass Spectral Analysis

Mass spectra of BTBE and NO_2-BTBE were acquired by electron impact ionization using an HP5985B GC−MS system (Hewlett-Packard, Palo Alto, CA) equipped with ChemStation software. Samples dissolved in methanol were placed in a Direct Insertion Probe, and the temperature was programmed from 50 to 340 °C at a rate of 30 °C/min. The mass window was set at 100−800 atomic mass units (amu). The mass spectrum of DiBTBE was acquired with an ElectroSpray apparatus using an AUTOSPEC MS System (MicroMass, Manchester, U.K.). The sample was dissolved in a methanol/water/acetic acid (50:50 with 1% acetic acid) solvent system and introduced into the mass spectrometer via a syringe pump. The mass window for detection of DiBTBE was set at 300−3000 amu.

Spectroscopic Analysis

UV−vis spectra were acquired using a Shimadzu UV1601 UV−vis spectrometer at a wavelength interval of 1 nm. Fluorescence spectra were recorded using a Shimadzu RF-5301 PC spectrofluorometer. Excitation and emission bandwidths were set at 1.5 nm.

Table 1: Spectral Characteristics of BTBE and Its Oxidation and Nitration Products[a]

	MW	mass spectra	UV−vis spectra	fluorescence spectra
N-*t*-BOC L-tyrosine *tert*-butyl ester (BTBE)	337	337 $(M)^+$, electron ionization	277 nm	ex = 281 nm, em = 306 nm
3′-nitro *N*-*t*-BOC L-tyrosine *tert*-butyl ester (NO_2-BTBE)	382	382 $(M)^+$, electron ionization	276 and 354 nm (pH 3.0), 282 and 424 nm (pH 12)	not available
3,3′-di *N*-*t*-BOC L-tyrosine *tert*-butyl ester (DiBTBE)	672	696 $(M + H + Na)^+$, electrospray	285 nm	ex = 294 nm, em = 401 nm

[a] All fluorescence and UV−vis spectra were recorded at pH 3.0 in a solution of 70% methanol and 15 mM phosphate buffer, except at pH 12 where the spectrum was recorded in a solution containing 70% methanol and 0.01 M NaOH.

ESR Spin Trapping

ESR spectra were recorded at room temperature on a Varian E-109 spectrometer operating at 9.5 GHz and using 100 kHz field modulation equipped with a TE_{102} cavity. Reactions were initiated by adding peroxynitrite to incubation mixtures containing 25 mM EMPO in various buffers or solvents. The decomposed peroxynitrite was made by incubating peroxynitrite in 90% *N*,*N*-dimethylformamide (DMF) for 15 min prior to the addition of EMPO. The samples were immediately transferred to a capillary tube that was sealed with a miniseal (Baxter Scientific Products, McGraw Park, IL) and placed inside a cavity, and spectra were immediately recorded. Spectrometer conditions were as follows: modulation amplitude, 1 G; time constant, 64 ms; scan time, 2 min; and microwave power, 10 mW. Typically, the spectra presented in this study were the average of three scans.

RESULTS

Spectral Properties of BTBE and Its Derivatives. Table 1 summarizes the optical, fluorescence, and mass spectral data of BTBE, NO_2-BTBE, and DiBTBE. These compounds were purified by HPLC procedures using a C-18 preparative column (Beckman, 10 mm × 250 mm, 5 μm). BTBE and NO_2-BTBE were clearly separated using a methanol gradient with the concentration increasing from 70 to 78% over the course of 100 min. The retention times for BTBE and NO_2-BTBE under these conditions were 35 and 56 min, respectively. DiBTBE was purified on the same column using a linear increase in methanol concentration from 77 to 80% over the course of 70 min. Under these HPLC conditions, the retention times for BTBE and DiBTBE were 22 and 60 min, respectively (data not shown).

Location of BTBE in the Bilayer: Fluorescence Quenching by Phospholipid Spin-Labels. BTBE fluorescence was significantly enhanced and slightly blue-shifted in the presence of liposomes (Figure 3A), indicating that it partitions into the hydrophobic phase of the bilayer. This is consistent with the very poor solubility of BTBE in aqueous solvents. BTBE fluorescence in liposomes was strongly quenched by nitroxide-labeled phospholipids in the order 5-PCSL > 16-PCSL > 12-PCSL (Figure 3B), and to a lesser extent by the water-soluble nitroxide, tempocholine (data not shown). The fact that the extent of fluorescence quenching by 16-PCSL falls between those of 5- and 12-PCSL is consistent with the known propensity of nitroxides located at the 16 position to fold back toward the membrane surface (*24*, *25*). These results show that BTBE is located in the lipid phase of the bilayer and suggest that it is distributed throughout the bilayer, with the highest concentration present near the glycerol backbone (i.e., at the level of 5-PCSL). Although tempocholine is primarily confined to the aqueous phase, it is quite likely that there is some penetration near the membrane surface in these neutral liposomes that lack cholesterol or other components to promote packing in the liquid crystalline phase.

ESR spectra of the PC spin-labels were not altered by the presence of BTBE (Figure 3C), indicating that the bilayer structure is not perturbed by this low level (i.e., 1 mol % relative to phospholipid) of the tyrosine analogue.

Peroxynitrite-Dependent Oxidation and Nitration of BTBE in Membranes and Tyrosine in Aqueous Solution. A bolus addition of peroxynitrite (50 μM) to DLPC liposomes containing BTBE (300 μM) resulted in the formation of a product eluting at 11 min as determined by HPLC with UV detection (Figure 4A, middle trace). This peak was assigned to the nitration product, NO_2-BTBE, by comparison with the authentic standard (Figure 4A, top trace). HPLC fluorescence analysis of the same mixture indicated a product with a retention time of 23 min (Figure 4B, middle trace), which was attributed to a dimeric oxidation product of BTBE, based on the HPLC profile of authentic DiBTBE (Figure 4B, top trace). Bolus addition of increasing concentrations of peroxynitrite significantly enhanced the formation of NO_2-BTBE (Figure 5A) without greatly affecting the yield of DiBTBE (Figure 5B). Under identical conditions, bolus addition of peroxynitrite to a phosphate buffer containing tyrosine (300 μM) also yielded both the nitrated and oxidized products (i.e., NO_2Tyr and DiTyr) as monitored by HPLC−UV and fluorescence detection. However, the yields of NO_2-Tyr and DiTyr (as measured by the area under the curve) were 2−3-fold higher than those of NO_2-BTBE and DiBTBE (panels A and B of Figure 5). At high peroxynitrite concentrations (~500 μM), the yield of DiTyr (Figure 5B) was actually diminished. We have previously shown that DiTyr can undergo oxidation and nitration reactions forming tri- and tetratyrosine and nitrodityrosine, respectively (*23*). On the basis of these results, we conclude that the extent of nitration of tyrosine and BTBE in the presence of peroxynitrite is nearly 50−100-fold higher than the extent of their oxidation reaction.

The addition of peroxynitrite in a slow infusion to DLPC liposomes containing BTBE or to phosphate buffer containing tyrosine gave, however, a different product profile. As shown in Figure 6, when peroxynitrite was infused at a rate of 2−10 μM/min, the yield of NO_2-BTBE was slightly higher than that of NO_2Tyr. However, in both cases, the yield of the oxidation products (i.e., DiBTBE and DiTyr) was considerably lower than that of the nitration products (Figure

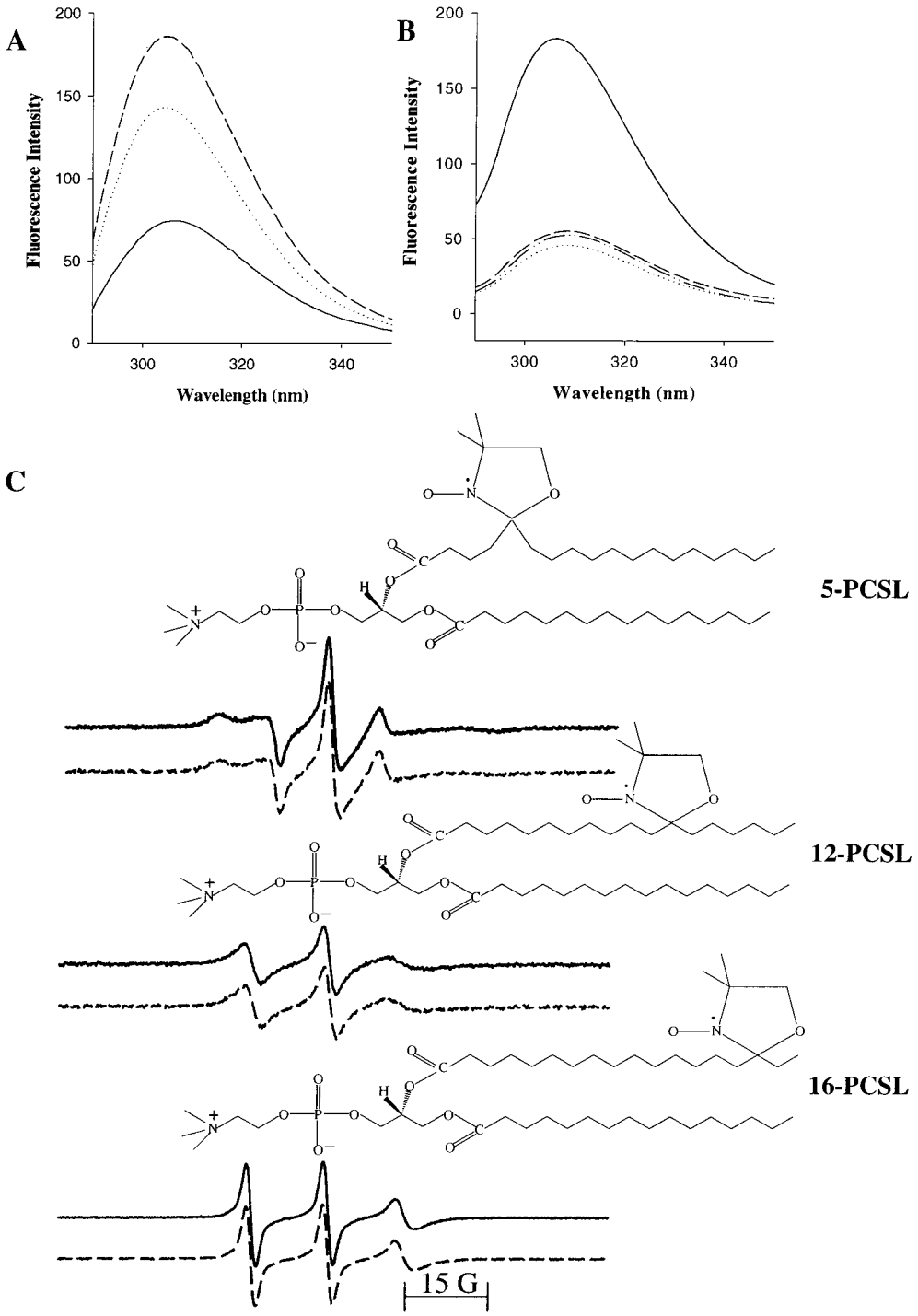

FIGURE 3: Fluorescence spectra of BTBE. (A) BTBE (0.3 mM) was dissolved in methanol (—) or cyclohexane (···) or incorporated into liposomes (30 mM) (– – –) in phosphate (0.1 M) buffer containing DTPA (0.1 mM, pH 7.4). (B) BTBE (0.3 mM) alone (—) or with 3 mM 5-doxyl (···), 12-doxyl (– – –), or 16-doxyl PCSL (—··—) was incorporated into DLPC liposomes (30 mM). (C) ESR spectra of 5-doxyl, 12-doxyl, and 16-doxyl PCSL (0.3 mM) after incorporation into DLPC liposomes (30 mM) alone (—) or DLPC liposomes (30 mM) containing BTBE (0.3 mM) (– – –). The ESR spectra were recorded using the following parameters: scan range, 100 G; central field, 3386 G; scan time, 120 s; time constant, 64 ms; microwave frequency, 9.51 GHz; and microwave power, 10 mW.

6A,B). More importantly, even during slow infusion of peroxynitrite, the yield of NO_2-BTBE was nearly 5 times higher than that of DiBTBE, the oxidation product of BTBE (Figure 6A). These data indicate that peroxynitrite-dependent nitration of the tyrosine probe is a predominant reaction in membranes as compared to the oxidation process yielding dityrosyl products. Two important pieces of information emerge from these results. (i) During bolus addition of peroxynitrite, the levels of both nitration and oxidation of tyrosine increased with increasing dose, and (ii) during slow infusion of peroxynitrite, the level of nitration but not oxidation of tyrosine increased. In addition, the findings presented here indicate that even at low infusion rates of peroxynitrite, nitration of tyrosine is more efficient than the oxidation reaction.

Peroxynitrite-Mediated Oxidation and Nitration Reactions of BTBE and Tyrosine: The Effect of Bicarbonate. To investigate the effect of peroxynitrite that is slowly infused

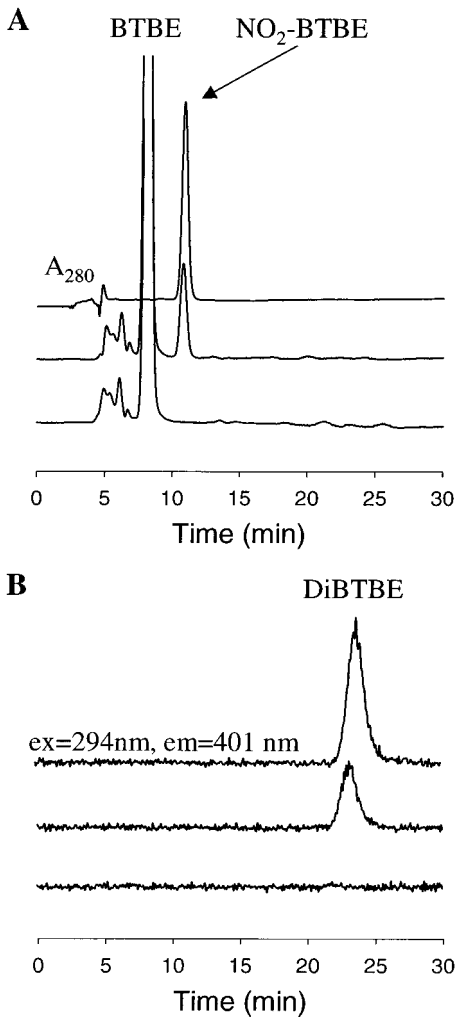

FIGURE 4: HPLC analysis of BTBE, NO_2-BTBE, and DiBTBE. (A) A typical HPLC trace of authentic NO_2-BTBE (25 μM) (top), an incubation mixture consisting of BTBE (0.3 mM) in DLPC (30 mM) liposomes and peroxynitrite (50 μM) (middle), and the same as above except without peroxynitrite (bottom). HPLC traces were monitored at 280 nm. (B) Authentic DiBTBE (2 μM) (top). The middle and bottom traces correspond to incubations identical to those for the middle and bottom traces shown in panel A, respectively. HPLC traces were followed by fluorescence analysis.

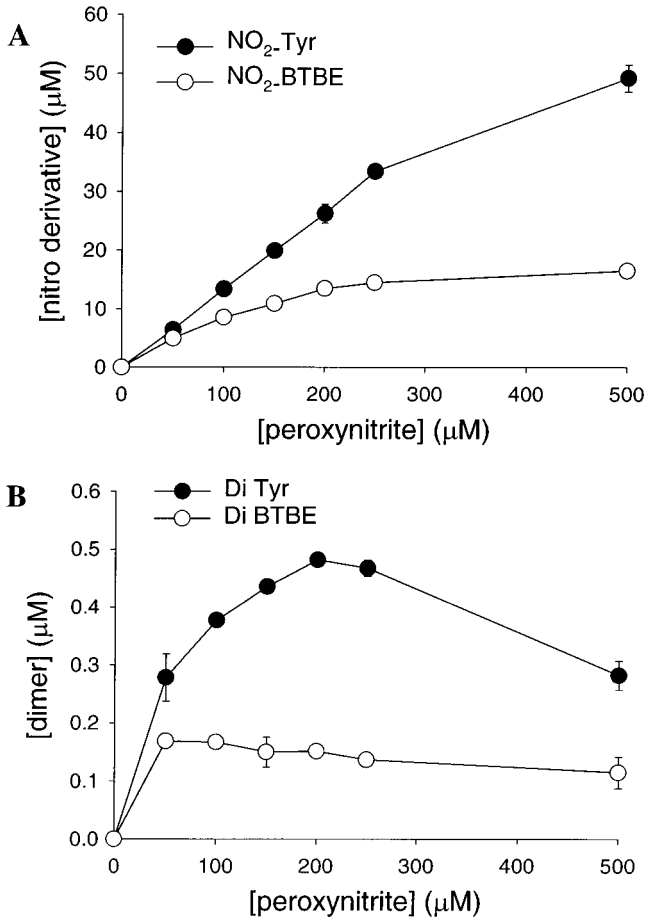

FIGURE 5: Nitration and oxidation of tyrosine in the aqueous phase and BTBE in membranes by a bolus addition of peroxynitrite. BTBE (0.3 mM) in DLPC (30 mM) liposomes was incubated with various amounts of peroxynitrite in sodium phosphate buffer (0.1 M, pH 7.4) and analyzed by HPLC ($n = 3 \pm$ SD). The comparable aqueous reaction was performed using tyrosine (0.3 mM). (A) Peroxynitrite concentration-dependent nitration and (B) peroxynitrite concentration-dependent oxidation. Note differences in the scale for nitration (A) and oxidation (B) products.

or cogenerated in situ on nitration and/or oxidation of BTBE in membranes and tyrosine in the aqueous solution, DLPC liposomes containing BTBE (300 μM) or tyrosine (300 μM in phosphate buffer) were incubated with SIN-1 (250, 500, and 1000 μM). Figure 7 shows that the level of nitration of BTBE in the membrane (Figure 7B) is greater than the level of nitration of tyrosine in aqueous solution (Figure 7A). Again the overall oxidation of tyrosine and BTBE in the presence of peroxynitrite was still a relatively minor reaction (Figure 8A,B). These results strongly suggest that nitration but not oxidation of tyrosyl residue is a dominant process of peroxynitrite-dependent reactions, especially in the membrane.

Bicarbonate anion (HCO_3^-) has been shown to enhance peroxynitrite-dependent oxidation and nitration of tyrosine (*26*−*31*). Peroxynitrite has been proposed to react with CO_2 to generate the nitrosoperoxycarbonate ($ONOOCO_2^-$) intermediate that presumably caused an increase in the levels of nitration and oxidation of tyrosine (see Scheme 1 in Discussion). Thus, we compared the effects of HCO_3^- on nitration and oxidation of BTBE in membranes with those of tyrosine in aqueous solution. As shown in Figures 7−9, HCO_3^- significantly enhanced the nitration and oxidation of tyrosine. In marked contrast, HCO_3^- had little or no effect on the nitration and oxidation reactions of BTBE (Figures 7B, 8B, and 9A,B). The relative lack of an effect of HCO_3^- on peroxynitrite-mediated oxidation and nitration reactions in membranes may be attributed to the lack of diffusion or slow diffusion of the intermediate radical pair ($NO_2^{\bullet}\cdots CO_3^{\bullet-}$) into membranes (see Scheme 1 in Discussion). At higher fluxes of $^{\bullet}NO$ and $O_2^{\bullet-}$, it is possible that other oxidation products of tyrosine are formed. Alternatively, peroxynitrite may also react with excess SIN-1. Both processes will lead to a decrease in the yield of dityrosine (Figure 8).

Spin Trapping Evidence for Hydroxyl Radical Adduct Formation from Peroxynitrite in Aprotic Solvents. Previously recorded spin trapping data with $ONOO^-$ had been obtained using 5,5-dimethyl-1-pyrroline *N*-oxide (DMPO) in aqueous solutions (*32*, *33*). In an attempt to probe the $ONOO^-$-dependent mechanism of nitration and oxidation of BTBE,

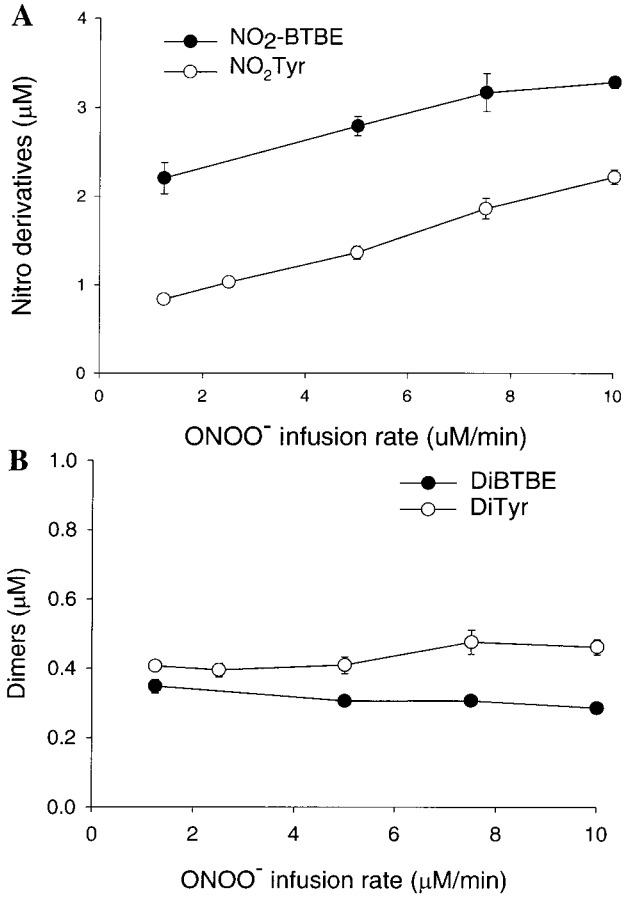

FIGURE 6: Nitration and oxidation of BTBE in membranes and tyrosine in the aqueous phase by a slow infusion of peroxynitrite. BTBE (0.3 mM) in DLPC liposomes (30 mM) was infused with peroxynitrite at different rates (final peroxynitrite concentration, 50 μM) in phosphate buffer (0.1 M, pH 7.4) and analyzed by HPLC. The corresponding aqueous reaction was performed using tyrosine (0.3 mM). (A) Peroxynitrite infusion rate-dependent nitration and (B) peroxynitrite infusion rate-dependent oxidation.

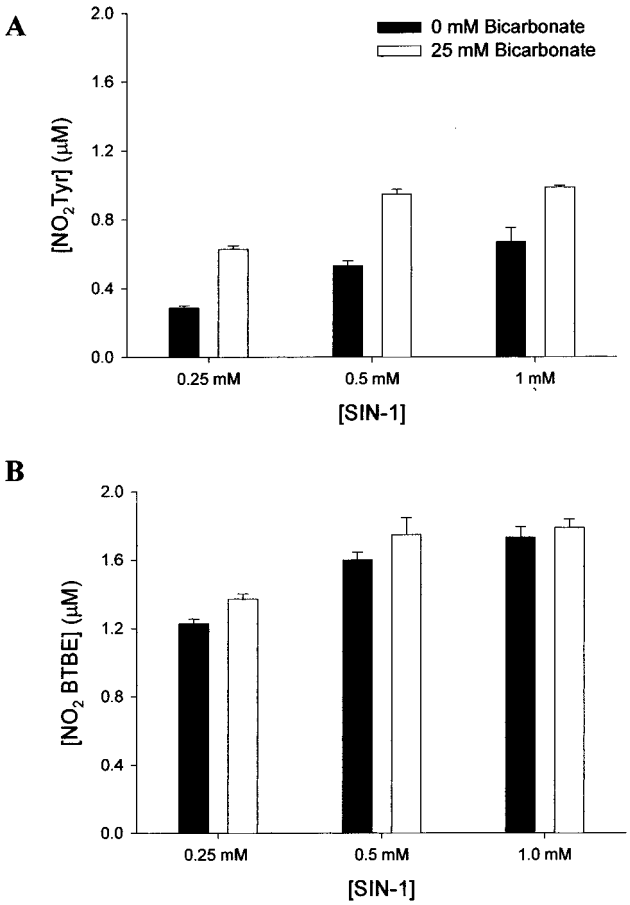

FIGURE 7: Nitration of tyrosine in aqueous solution and BTBE in membranes by SIN-1. BTBE (0.3 mM) in DLPC (30 mM) liposomes was incubated with SIN-1 and bicarbonate (0 or 25 mM) in sodium phosphate buffer (0.1 M, pH 7.4) and analyzed by HPLC ($n = 3 \pm$ SD). The comparable aqueous reaction was performed using tyrosine (0.3 mM). (A) Nitration in the aqueous phase and (B) nitration in membranes.

we used electron spin resonance (ESR) spin trapping with a lipophilic, membrane-incorporated nitrone spin trap, α-phenyl-*tert*-butyl-*N*-nitrone (PBN). Unfortunately, no ESR spectrum of the spin adduct corresponding to the PBN−hydroxyl adduct was detected as PBN−oxy radical adducts are very unstable (*34*). To better understand $ONOO^-$ decomposition in a hydrophobic environment, we used aprotic solvents, such as dimethylformamide (DMF) or dimethyl sulfoxide (DMSO). Hydroxyl radicals do not appreciably react with DMF to generate secondary radicals, while DMSO reacts with hydroxyl radicals to form methyl radicals (which can be trapped to form a more persistent spin adduct) and other products (*35*, *36*). We employed two spin traps, EMPO and DBNBS, to investigate radical formation from peroxynitrite. In aqueous solution, $ONOO^-$ rapidly destroyed hydroxyl spin adducts. To minimize this, spin trapping reactions were previously carried out in the presence of reductants such as glutathione (*32*).

The addition of peroxynitrite (3 mM) to a DMF/water mixture containing 25 mM EMPO generated the ESR spectrum (Figure 10A) of a diastereomeric mixture of EMPO−OH adducts [$\alpha_N = 13.5$ G, $\alpha^{\beta}_H = 14.8$ G, and $\alpha^{\gamma}_H = 0.8$ G (52%); $\alpha_N = 13.5$ G and $\alpha^{\beta}_H = 12.4$ G (48%)] (*20*, *37*). Decomposed peroxynitrite did not yield any ESR spectrum (Figure 10C), nor did a DMF/water mixture containing H_2O_2 and nitrite (data not shown). The authentic EMPO−OH adduct generated using a Fenton reaction (H_2O_2/Fe^{2+}) in a DMF/H_2O mixture yielded an ESR spectrum (Figure 10E) that is identical to Figure 10A. On the basis of these findings, the spectra (Figure 10A,E) were attributed to the hydroxyl adduct of EMPO.

To investigate whether free hydroxyl radicals are formed from the decomposition of peroxynitrite, we used a DMSO/H_2O mixture. Peroxynitrite readily reacts with most hydroxyl radical scanvengers, but the reaction between DMSO and peroxynitrite has previously been used to monitor hydroxyl formation (*33*, *36*). The water-soluble nitroso spin trap, DBNBS, had been used to detect methyl radicals formed in cellular and enzymatic systems (*38*). The resulting DBNBS−methyl radical adduct (DBNBS−CH_3) is more persistent and exhibits a highly characteristic ESR spectrum. Addition of peroxynitrite to a DMSO/H_2O mixture containing 25 mM DBNBS and DTPA (100 μM) produced an ESR spectrum of the DBNBS−CH_3 adduct [$\alpha_N = 14.1$ G, $\alpha_H = 13.5$ G, and $\alpha_{H(m)} = 0.7$ G] (Figure 11A). In the presence of decomposed peroxynitrite, the spectral intensity of the DBNBS−CH_3 adduct was significantly decreased (Figure 11B). Figure 11C shows the ESR spectrum of an authentic DBNBS−CH_3 adduct formed from the Fenton reaction (Fe^{2+}

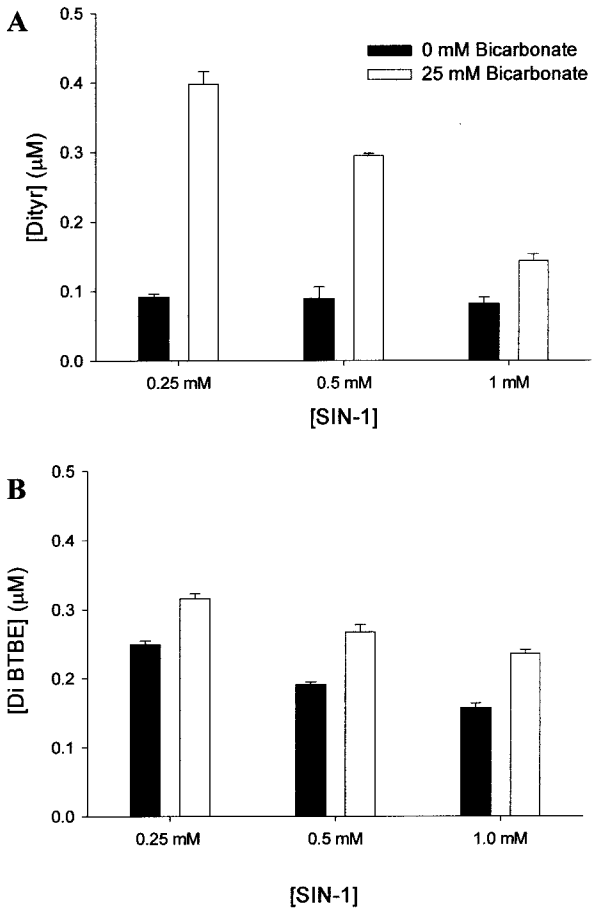

FIGURE 8: Oxidation of tyrosine in aqueous solution and BTBE in membranes by SIN-1. BTBE (0.3 mM) in DLPC (30 mM) liposomes was incubated with SIN-1 and bicarbonate (0 or 25 mM) in sodium phosphate buffer (0.1 M, pH 7.4) and analyzed by HPLC ($n = 3 \pm$ SD). The comparable aqueous reaction was performed using tyrosine (0.3 mM). (A) Oxidation in the aqueous phase and (B) oxidation in membranes.

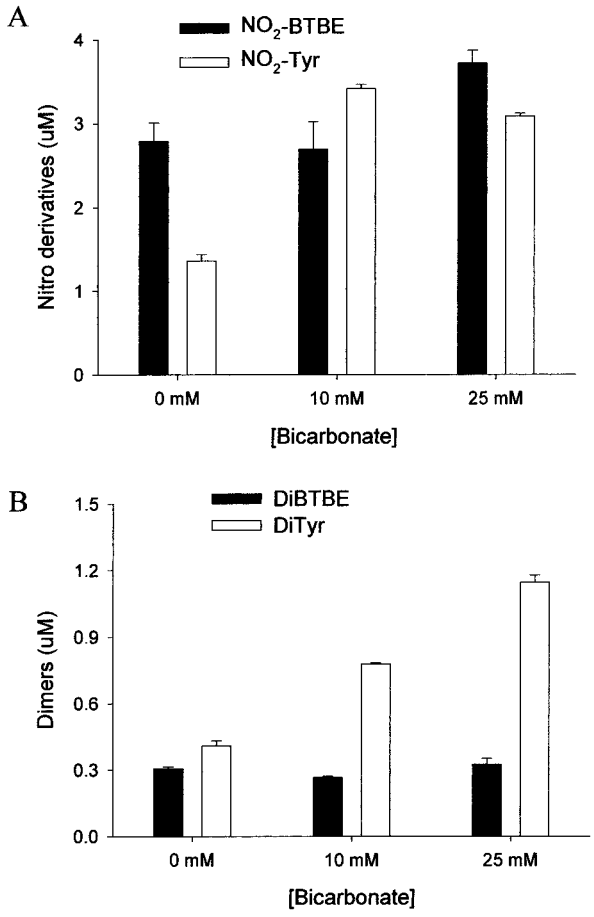

FIGURE 9: Bicarbonate effects on the nitration and oxidation of BTBE and tyrosine by slow infusion of peroxynitrite. BTBE (0.3 mM) in DLPC (30 mM) liposomes was infused with peroxynitrite at a rate of 5 μM/min (final peroxynitrite concentration, 50 μM) in sodium phosphate buffer (0.1 M, pH 7.4) with various amounts of bicarbonate. The comparable aqueous reaction was carried out using tyrosine (0.3 mM). The data represented three to four repeats $\pm$ the standard error of the mean. (A) Bicarbonate effects on nitration and (B) bicarbonate effects on oxidation.

$+ H_2O_2 \rightarrow Fe^{3+} + {}^{\bullet}OH + {}^{-}OH$), where methyl radicals are formed from the reaction between DMSO and $^{\bullet}OH$. These results demonstrate unambiguously that the decomposition of peroxynitrite in aprotic solvent generates free hydroxyl radicals. In the presence of 10 mM bicarbonate, the formation of the DBNBS$-CH_3$ adduct is considerably inhibited (Figure 11D), clearly indicating that peroxynitrite does not decompose to form $^{\bullet}OH$ in the presence of CO_2. This observation is consistent with the previous report (*33*).

DISCUSSION

Nitration of the Transmembrane Tyrosyl Probe. Previously, we showed that both SIN-1 and peroxynitrite preferentially nitrated membrane-bound γ-tocopherol instead of tyrosine in aqueous solution (*15*). γ-Tocopherol underwent nitration at the 5 position of the chromanol ring to form 5-NO_2-γ-tocopherol. This finding raised important questions with respect to the mechanisms of phenolic nitration by peroxynitrite in the hydrophobic phase. Unlike trolox, which is a water-soluble analogue of α-tocopherol, there exists no water-soluble analogue of γ-tocopherol. Therefore, we were not able to directly compare the nitrating efficiency of peroxynitrite in the aqueous and hydrophobic phases using γ-tocopherol. Consequently, we compared the nitrating and oxidizing reactions of peroxynitrite using tyrosine probes. Tyrosine methyl and ethyl esters (Table 2) were not suitable for this purpose as they underwent slow hydrolysis to form tyrosine. Although tyrosine butyl ester was resistant to hydrolysis, its level of incorporation into liposome was only 53%. As shown in Table 2, BTBE was almost totally incorporated into liposomes, and was resistant to hydrolysis for at least 40 h. For these reasons, BTBE appeared to be an ideal hydrophobic tyrosyl probe for investigating nitration and oxidation reactions in membranes.

Another advantage of using a membrane-bound tyrosyl probe to detect reactive nitrogen species is that the nitrated tyrosyl probe does not undergo biological reduction. Incubation of NO_2-BTBE (300 μM) in DLPC liposomes in the presence of the xanthine/xanthine oxidase system did not cause a significant reduction in the level of NO_2-BTBE. In contrast, nitrotyrosine underwent a significant level reduction in the presence of xanthine and xanthine oxidase (unpublished data). Recently, it has been reported that nitroreductases present in the cytosol cause nitro reduction (*42*), although the proposed reaction mechanism has recently been questioned (*1*).

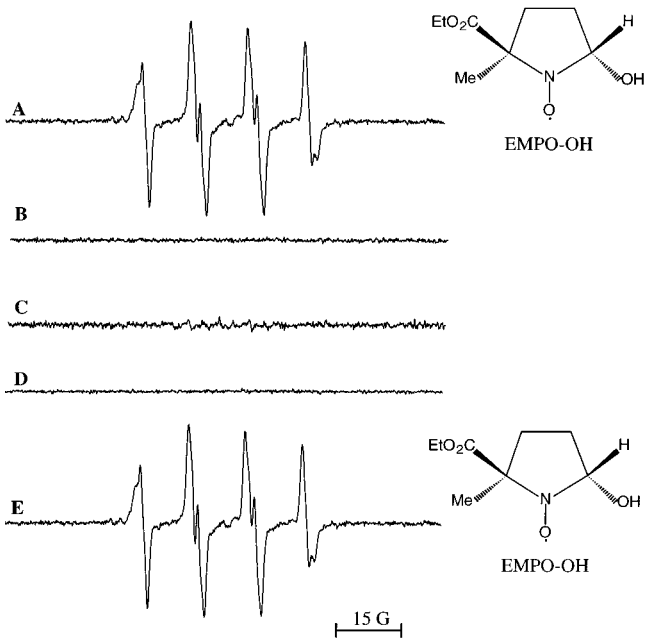

FIGURE 10: EMPO−hydroxyl radical adduct formation in a 90% DMF/H_2O mixture. Peroxynitrite (3 mM) was mixed with EMPO (25 mM) in (A) a 90% DMF/10% H_2O mixture with the pH adjusted with HCl to 7−8. (B) Phosphate buffer (0.1 M, pH 7.4) and DTPA (100 μM). (C) Decomposed peroxynitrite. (D) H_2O_2 (3 mM) and $NaNO_2$ (3 mM). (E) H_2O_2 (3 mM) and $FeSO_4$ (0.1 mM).

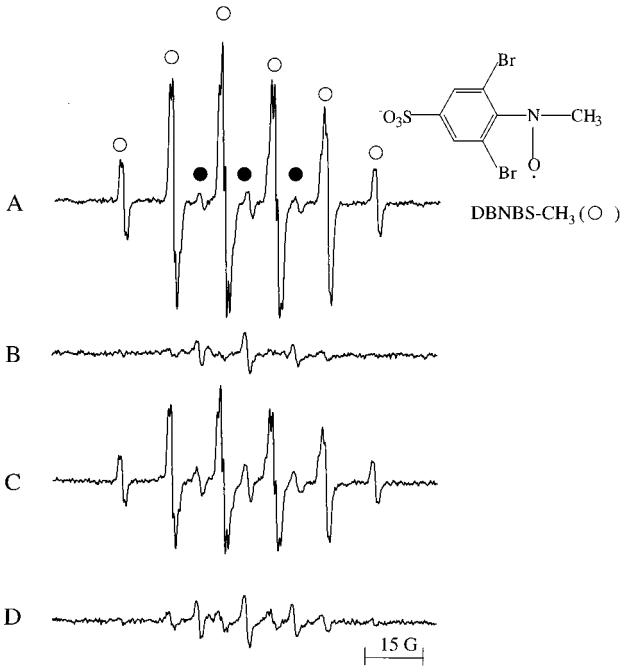

FIGURE 11: DBNBS−methyl radical adduct formation. (A) Peroxynitrite (2 mM) was mixed with 25 mM DBNBS in 50% DMSO containing 50 mM phosphate buffer and 100 μM DTPA. (B) Same as panel A except that peroxynitrte was preincubated with buffer and solvent for 15 min before addition of DBNBS. (C) Hydrogen peroxide (1 mM) and $FeSO_4$ (0.1 mM) in the same solvent/buffer system as panel A. (D) Same as panel A except with 10 mM bicarbonate. Spectral lines represented by solid circles correspond a contaminating nitroxide impurity, and the lines denoted by open circles are attributed to the DBNBS−CH_3 adduct.

Mechanism of Nitration and Oxidation of the Membrane-Bound Tyrosyl Probe. Peroxynitrite exists in equilibrium with peroxynitrous acid as follows (*37*):

$$\mathrm{ONOOH} \underset{\mathrm{H^+}}{\overset{\mathrm{p}K_a=6.8}{\rightleftharpoons}} \mathrm{ONOO^-}$$

Both $ONOO^-$ and ONOOH were reported to cross the lipid membrane through an ion transport channel or passive diffusion at rates similar to that of water (*16*, *17*). Homolytic cleavage of ONOOH into hydroxyl radical ($^{\bullet}OH$) and nitrogen dioxide radical ($NO_2^{\bullet}$), a potent nitrating agent, was originally believed to be the mechanism responsible for the free radical-like activity of peroxynitrite (*32*, *33*). Other proposed mechanisms exist for the nitration of tyrosine by peroxynitrite, including the formation of a nitronium-like intermediate (*39*) or direct oxidation of tyrosine by peroxynitrite via a rapid consecutive one-electron oxidation reaction without the involvement of $NO_2^{\bullet}$ or $^{\bullet}OH$ (*40*). The lack of involvement of $^{\bullet}OH$ in tyrosine nitration was supported by the inability to quench nitration reactions by hydroxyl radical scavengers (*40*).

The data presented here unequivocally show that the level of nitration of BTBE in membranes far exceeds the level of oxidation of BTBE. Formation of DiTyr is usually a key indicator of tyrosyl radical-mediated mechanisms (*26*, *27*). As has been previously reported (*26*, *27*), HCO_3^- significantly enhanced peroxynitrite-mediated nitration and dimerization of tyrosine in aqueous solution. This can be attributed to the intermediacy of the carbonate radical ($CO_3^{\bullet-}$), which facilitates the one-electron oxidation of tyrosine (Scheme 1) (*41*). HCO_3^-, however, did not significantly enhance nitration and oxidation reactions in membranes. This is probably due to the lack of formation of the nitrosoperoxycarbonate ($ONOOCO_2^-$) intermediate in the membrane, or to the slow diffusion of $ONOOCO_2^-$ into the membrane. Previous reports indicate that HCO_3^- actually inhibited nitration and oxidation of γ- and α-tocopherols (*15*). A more recent report also elaborated on this aspect (*46*).

Nitration of Tyrosine in Proteins. All the factors responsible for peroxynitrite-mediated nitration of tyrosine residue(s) in proteins are not completely understood. However, some aspects of nitration of specific protein targets are emerging (*1*). It is now recognized that the number of tyrosine residues per se does not necessarily determine the extent of target protein modification by nitration (*1*). It has been suggested that the presence of glutamate adjacent to the tyrosyl residues influences tyrosine nitration. Tyrosine in the protein side chain has a hydrophobicity value of about −1.47 kcal/mol (*1*), approximately in the middle of the hydrophobicity scale of amino acids.

The effect of HCO_3^- on peroxynitrite-mediated nitration of protein tyrosine should be taken into consideration. On the basis of the data presented here, one would predict that HCO_3^- will enhance nitration of tyrosyl residues exposed to the aqueous phase and inhibit nitration of tyrosine in a hydrophobic environment. Additional research on the structural biology of nitrated proteins may yield further insight with regard to the nitrating species responsible for peroxynitrite-mediated tyrosine nitration and the relative susceptibility of different tyrosine residues in a membrane protein. Recently, tyrosines present in the transmembrane domain of sarcoplasmic reticulum Ca^{2+}-ATPase were shown to undergo a selective nitration (*47*).

Table 2: Stability and Incorporation of Tyrosine Esters in Liposomes

tyrosine ester	stability[a] incubation mixture	incubation time (h)	recovery (%)	percent incorporation[b] into liposome
tyrosine methyl ester	phosphate buffer (0.1 M, pH 7.4)	8	69	not applicable
tyrosine ethyl ester	phosphate buffer (0.1 M, pH 7.4)	8	86	not applicable
tyrosine *tert*-butyl ester	phosphate buffer (0.1 M, pH 7.4)	8	100	53
BTBE	methanol	40	100	98
	70% methanol and phosphate buffer (15 mM, pH 3.0)	40	100	

[a] Tyrosine esters were dissolved in the solvents as specified in the table and immediately injected into the HPLC system. After incubation at room temperature for a certain period of time, the samples were analyzed by HPLC again. Recovery (%) = $(\text{peak area})_t/(\text{peak area})_{t=0} \times 100$. [b] Liposomes prepared to contain the various tyrosine esters were centrifuged at 14000*g* for 30 min, and the concentration of tyrosine ester remaining in the aqueous phase (Tyr_a) was measured at 280 nm in the presence of methanol (1:2, v/v). The total concentration of tyrosine ester in liposome (Tyr_t) was measured at A_{280} from a solution of liposome dissolved in methanol (1:2, v/v). The tyrosine incorporated into membrane (%) = $[(Tyr_t) - (Tyr_a)]/(Tyr_t) \times 100$.

Scheme 1: Postulated Reaction Pathways for Nitration and Oxidation of a Hydrophobic Tyrosine Analogue in Membranes by Peroxynitrite

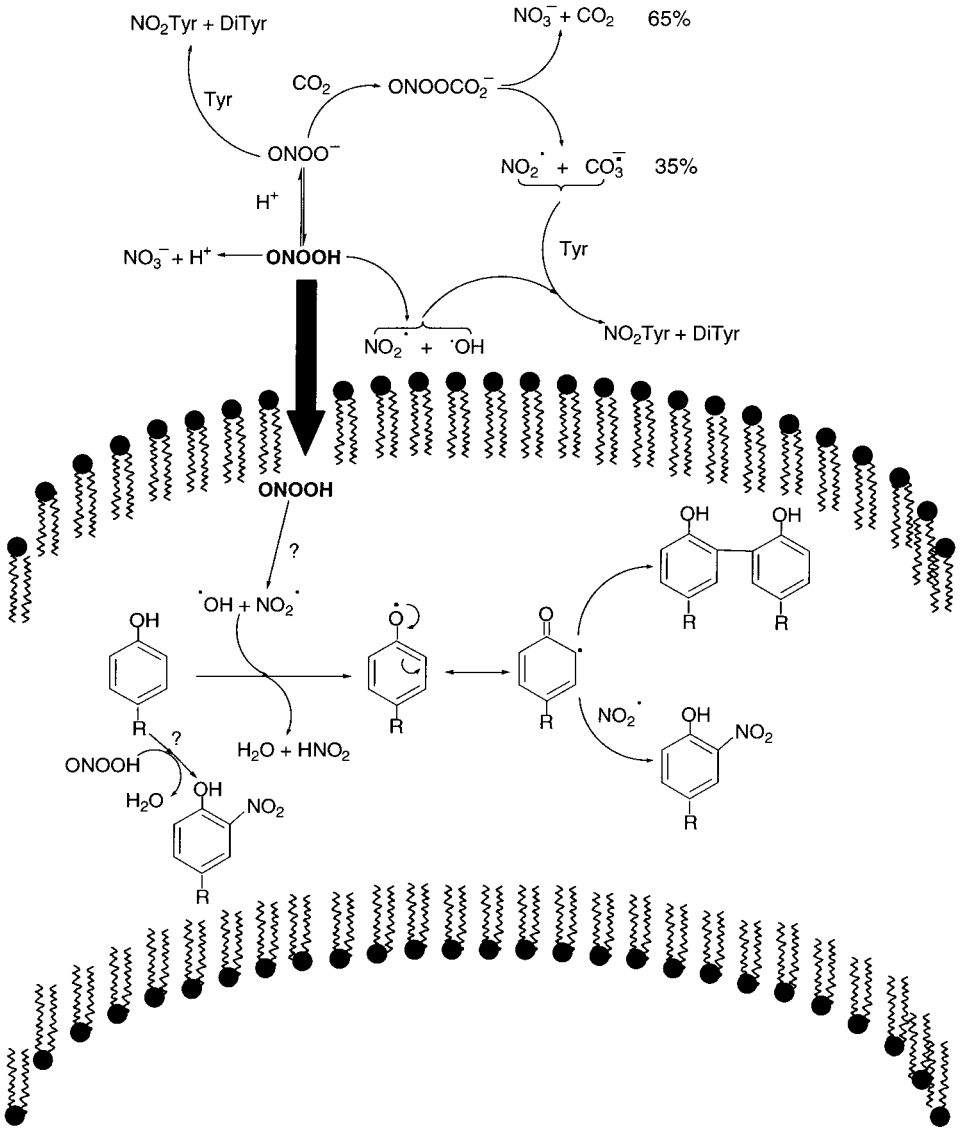

SUMMARY

Peroxynitrite, preformed or generated in situ from the reaction between •NO and $O_2^{\bullet-}$, was shown to be responsible for nitration of tyrosine in the aqueous phase (*48*−*50*). We have shown in this study that preformed peroxynitrite, added as a bolus or generated simultaneously at low levels from independent sources of •NO and $O_2^{\bullet-}$, causes nitration as a predominant reaction in membranes. Recently, the oxidation of the tyrosine moiety to the dityrosyl product is not a significant reaction process in the case of the membrane-incorporated tyrosine analogue. In the presence of HCO_3^-, the reaction mechanism in the aqueous phase switches to a

radical process through formation of a peroxynitrosocarbonate intermediate. Although HCO_3^- greatly amplified aqueous solution nitration and oxidation of tyrosine, it did not greatly affect oxidation and nitration of the membrane-bound tyrosine.

As shown in this study and in an earlier report (*15*), SIN-1, which produces simultaneously both $^{\bullet}NO$ and $O_2^{\bullet-}$ at the same rate, preferentially nitrated membrane-associated γ-tocopherol and BTBE. However, SIN-1 did not cause nitration of aqueous tyrosine. It has been suggested that the lack of nitration of tyrosine by cogenerated $^{\bullet}NO$ and $O_2^{\bullet-}$ is predominantly controlled by the rapid reaction between $O_2^{\bullet-}$ and the tyrosyl phenoxyl radical (*28*). This reaction rate is comparable to the rate of the reaction of $^{\bullet}NO$ with $O_2^{\bullet-}$ (*43*). With the hydrophobic tyrosyl substrates or γ-tocopherol, it is likely that the reaction between $O_2^{\bullet-}$ and membrane-bound phenoxyl radicals is restricted. As a result, nitration occurs through a recombination reaction mechanism between the membrane-incorporated tyrosyl radical and $NO_2^{\bullet}$. Furthermore, $NO_2^{\bullet}$ undergoes hydrolysis quite readily in aqueous solution, but in the hydrophoblic phase, $NO_2^{\bullet}$ is more likely to be involved in the nitration and oxidation reaction (*44*), as illustrated in Scheme 1.

Formation of the dityrosine oxidation product requires a bimolecular reaction between two tyrosyl phenoxyl radicals (Scheme 1). While this can be a facile reaction in solution where translational diffusion is fast, it will be strongly impeded in a membrane bilayer where lateral diffusion is at least an order magnitude slower relative to the aqueous phase even for feely diffusing lipids and tocopherols. Lateral diffusion of integral membrane proteins is further restricted (*45*), making nitration by peroxynitrite an even more likely outcome. Consequently, under the physiological conditions of relatively low peroxynitrite concentrations, the local environment of target tyrosine residues may play a key role in determining whether oxidation or nitration occurs with nitration predominating in membranes and at sites buried in the protein tertiary structure.

This study demonstrates preferential nitration of a tyrosine analogue that is distributed throughout the hydrophobic phase of the bilayer. Further studies to more accurately mimic the reactivity of tyrosyl side chains in membrane proteins using peptides with tyrosine residues anchored at specific depths in the bilayer are in progress.

ACKNOWLEDGMENT

We sincerely thank Dr. Frank E. Laib for obtaining the mass spectra of compounds.

REFERENCES

1. Ischiropoulos, H. (1998) *Arch. Biochem. Biophys. 356*, 1−11.
2. Van der Vliet, A., Eiserich, J. P., O'Neill, C. A., Halliwell, B., and Cross, C. E. (1995) *Arch. Biochem. Biophys. 319*, 341−349.
3. Prutz, W. A., Monig, H., Butler, J., and Land, E. J. (1985) *Arch. Biochem. Biophys. 243*, 125−134.
4. Leeuwenburgh, C., Hardy, M. M., Hazen, S. L., Wagner, P., Oh-ishi, S., Steinbrecher, U. P., and Heinecke, J. W. (1997) *J. Biol. Chem. 272*, 1433−1436.
5. Eiserich, J. P., Hristova, M., Cross, C. E., Jones, A. D., Freeman, B. A., Halliwell, B., and van der Vliet, A. (1998) *Nature 391*, 393−397.
6. Beckmann, J. S., Ye, Y. Z., Anderson, P. G., Chen, J., Accavitti, M. A., Tarpey, M. M., and White, C. R. (1994) *Biol. Chem. Hoppe-Seyler 375*, 81−88.
7. Buttery, L. D., Springall, D. R., Chester, A. H., Evans, T. J., Standfield, E. N., Parums, D. V., Yacoub, M. H., and Polak, J. M. (1996) *Lab. Invest. 75*, 77−85.
8. Bruijn, L. I., Beal, M. F., Becher, M. W., Schulz, J. B., Wong, P. C., Price, D. L., and Cleveland, D. W. (1997) *Proc. Natl. Acad. Sci. U.S.A. 94*, 7606−7611.
9. Kaur, H., and Halliwell, B. (1994) *FEBS Lett. 350*, 9−12.
10. Smith, M. A., Richey-Harris, P. L., Sayre, L. M., Beckman, J. S., and Perry, G. (1997) *J. Neurosci. 17*, 2653−2657.
11. Pfeiffer, S., and Mayer, B. (1998) *J. Biol. Chem. 273*, 27280−27285.
12. Pfeiffer, S., Schmidt, K., and Mayer, B. (2000*) J. Biol. Chem. 275*, 6346−6352.
13. Souza, J. M., Daikhin, E., Yudkoff, M., Raman, C. S., and Ischiropoulos, H. (1999) *Arch. Biochem. Biophys. 371*, 169−178.
14. Ohshima, H., Celan, I., Chazotte, L., Pignatelli, B., and Mower, H. F. (1999) *Nitric Oxide 3*, 132−141.
15. Goss, S. P. A., Hogg, N., and Kalyanaraman, B. (1999) *Arch. Biochem. Biophys. 363*, 333−340.
16. Marla, S. S., Lee, J., and Groves, J. T. (1997) *Proc. Natl. Acad. Sci. U.S.A. 94*, 14243−14248.
17. Groves, J. T. (1999) *Curr. Opin. Chem. Biol. 3*, 226−235.
18. Denicola, A., Souza, J. M., and Radi, R. (1998) *Proc. Natl. Acad. Sci. U.S.A. 95*, 3566−3571.
19. Malencik, D. A., Sprouse, J. F., Swanson, C. A., and Anderson, S. R. (1996) *Anal. Biochem. 242*, 202−213.
20. Papée, H. M., and Petriconi, G. L. (1964) *Nature 204*, 142−144.
21. Zhang, H., Joseph, J., Vásquez-Vivar, J., Karoui, H., Nsanzumuhire, C., Martásek, P., Tordo, P., and Kalyanaraman, B. (2000) *FEBS Lett. 473*, 58−62.
22. Kaur, H., Leung, K. H. W., and Perkins, M. J. (1981) *J. Chem. Soc., Chem. Commun.*, 142−143.
23. Zhang, H., Joseph, J., Felix, C., and Kalyanaraman, B. (2000) *J. Biol. Chem. 275*, 14038−14045.
24. Feix, J. B., Popp, C. A., Venkatramu, S. D., Park, J. H., and Hyde, J. S. (1984) *Biochemistry 23*, 2293−2299.
25. Feix, J. B., Yin, J.-J., and Hyde, J. S. (1987) *Biochemistry 26*, 3850−3855.
26. Lymar, S. V., and Hurst, J. K. (1995) *J. Am. Chem. Soc. 117*, 8867−8868.
27. Lymar, S. V., Jiang, Q., and Hurst, J. K. (1996) *Biochemistry 35*, 7855−7861.
28. Goldstein, S., Czapski, G., Lind, J., and Merenyi, G. (2000) *J. Biol. Chem. 275*, 3031−3036.
29. Goldstein, S., and Czapski, G. (1998) *J. Am. Chem. Soc. 120*, 3458−3463.
30. Uppu, R. M., Squadrito, G. L., and Pryor, W. A. (1996) *Arch. Biochem. Biophys. 327*, 335−343.
31. Denicola, A., Freeman, B. A., Trujillo, M., and Radi, R. (1996) *Arch. Biochem. Biophys. 333*, 49−58.
32. Augusto, O., Gatti, R. M., and Radi, R. (1994) *Arch. Biochem. Biophys. 310*, 118−125.
33. Gatti, R., Alvarez, M., Vásquez-Vivar, J., Radi, R., and Augusto, O. (1998) *Arch. Biochem. Biophys. 349*, 36−46.
34. Kotake, Y., and Janzen, E. G. (1991) *J. Am. Chem. Soc. 113*, 9503−9506.
35. Burkitt, M. J., and Mason, R. P. (1991) *Proc. Natl. Acad. Sci. U.S.A. 88*, 8440−8444.
36. Richeson, C. E., Mulder, P., Bowey, V. W., and Ingold, K. U. (1998) *J. Am. Chem. Soc. 120*, 7211−7219.
37. Olive, G., Mercier, A., Le Moigne, F., Rockenbauer, A., and Tordo, P. (2000) *Free Radical Biol. Med. 28*, 403−408.
38. Athar, M., Mukhtar, H., Bickers, D. R., Khan, I. U., and Kalyanaraman, B. (1989) *Carcinogenesis 10*, 1499−1503.

39. Koppenol, W. H., Moreno, J. J., Pryor, W. A., Ischiropoulos, H., and Beckman, J. S. (1992) *Chem. Res. Toxicol. 5*, 834−842.
40. Beckman, J. S., Ischiropoulos, H., Zhu, L., van der Woerd, M., Smith, C., Chen, J., Harrison, J., Martin, J. C., and Tsai, M. (1992) *Arch. Biochem. Biophys. 298*, 438−445.
41. Santos, C. X. C., Bonini, M. G., and Augusto, O. (1998) *Arch. Biochem. Biophys. 377*, 146−152.
42. Kamisaki, Y., Wada, K., Bian, K., Balabanli, B., Davis, K., Martin, E., Behbod, F., Lee, Y. C., and Murad, F. (1998) *Proc. Natl. Acad. Sci. U.S.A. 95*, 11584−11589.
43. Huie, R. E., and Padmaja, S. (1993) *Free Radical Res. Commun. 18*, 195−199.
44. Liu, X., Miller, M. J. S., Joshi, M. S., Thomas, D. D., and Lancaster, J. R., Jr. (1998) *Proc. Natl. Acad. Sci. U.S.A. 95*, 2175−2179.
45. Gennis, R. B. (1989) in *Biomembranes: Molecular Structure and Function*, Springer-Verlag, New York.
46. Khairutdinov, R. F., Coddington, J. W., and Hurst, J. K. (2000) *Biochemistry 39*, 14238−14249.
47. Viner, R. I., Ferrington, D. A., Williams, T. D., Bigelow, D. J., and Schoneich, C. (1999) *Biochem. J. 340*, 657−669.
48. Reiter, C. D., Teng, R., and Beckman, J. S. (2000) *J. Biol. Chem. 275*, 32460−32466.
49. Sawa, T., Akaike, T., and Maeda, H. (2000) *J. Biol. Chem. 275*, 32467−32474.
50. Masuda, M., Mower, H. F., Pignatelli, B., Celan, I., Friesen, M. D., Nishino, H., and Ohshima, H. (2000) *Chem. Res. Toxicol. 13*, 301−308.

BI002958C